Neutron Total Cross Sections in the 17- to 29-Mev Region*

J. M. PETERSON, A. BRATENAHL, AND J. P. STOERING
Lawrence Radiation Laboratory, University of California, Livermore, California
(Received February 18, 1960)

The neutron total cross sections of 42 elements and isotopes were measured at several energies between 17 and 29 Mev using monoenergetic neutrons produced by the Livermore variable-energy cyclotron through the $T(d,n)He^4$ reaction. Beam contaminations by gamma rays and low-energy "breakup" neutrons were measured by time-of-flight techniques, and their effects were kept small by suitably high bias on the plastic scintillator detector. The accuracy in cross section is typically ± 1 to 2%. The data in this energy region have been sparse heretofore. Where comparisons with previous data have been possible, there is substantial agreement. When plotted versus energy and mass number, the data form a smooth cross-section surface which joins on smoothly to the data at lower energies. The data seem in good agreement with the predictions of the optical model of Bjorklund and Fernbach.

INTRODUCTION

A SERIES of measurements of neutron total cross sections of 42 elements and isotopes has been made in the neutron energy range 17 to 29 Mev. This work is a continuation of similar experiments in the 7- to 14-Mev region which we published in 1958 in a paper[1] we shall herein refer to as P7-14. The motivation for this work was both to provide more and better data in a rather sparsely populated region and to help test the optical model[2] of the nucleus and evaluate its energy-dependent parameters.

APPARATUS

Our experiment consists of measuring the transmission of monoenergetic neutrons in good geometry, the usual method of measuring total cross sections. The neutrons are produced by the $d-T$ reaction using deuterons supplied by the Livermore 90-inch variable-energy cyclotron. The experimental equipment has been described in detail in P7-14. The collimated beam of deuterons strikes a tritium gas target after passing through a thin (9 to 18 mg cm^{-2}) tantalum entrance foil. A beam of neutrons from the gas target is defined by the neutron collimator which consists of a hole in a rectangular iron block two feet in length imbedded in a concrete mass. The transmission sample to be measured is positioned on the axis of the collimated neutron beam so as to shadow the detector. The positioning of the sample is accomplished by a movable, ten-position sample carriage. The iron and concrete collimator assembly prevents variable in-scattering from other nearby samples and from components of the carriage and serves also to reduce the general background.

Seven new transmission samples, including one rare earth, were added to the list reported in P7-14. The sample lengths are about 2 mean free paths (at 14 Mev), as prescribed by a calculation (Appendix II, P7-14) showing that for moderate background conditions this sample length minimizes the total running time for a given statistical error. The alignment of the detector, transmission sample, collimator, and gas target is done optically. The positioning of the samples can be controlled remotely with an accuracy of 0.008 in. A misalignment of at least 0.050 in. is found to be necessary to increase the transmission by 1%.

The electronic networks for the detector and monitor are identical, including temperature-stabilized preamplifiers and photomultiplier tubes. The detector is a cylindrical plastic scintillator $\frac{3}{4}$ in. in diameter and 1 in. in length. It is located 30 in. behind the sample and 90 in. from the gas target. The monitor is placed directly above the exit end of the collimator. It differs from the detector only in the shape of the plastic scintillator, a $\frac{3}{4}$-in. plastic sphere.

PROCEDURE

In addition to the neutrons of interest from the $T(d,n)He^4$ reaction, low-energy neutrons from $T(d,np)T$ and $T(d,2n)He^3$ breakup modes[3] provide an unwanted beam contaminant which increases with increasing deuteron energy. Another beam contaminant consists of gamma rays originating at or near the target.

The bias settings for the detector and monitor are determined by preliminary experiments in which the detected beam components are separated by the time-of-flight method. The time spectrum in Fig. 1 shows the detected components in the nominal 29-Mev neutron beam at two bias settings. The peak of the breakup neutrons corresponds to an energy of 7.5 Mev. The experimental bias for a given energy is chosen by examining the ratio of the detected contaminants to the

* This work was performed under auspices of the U. S. Atomic Energy Commission.

[1] A. Bratenahl, J. M. Peterson, and J. P. Stoering, Phys. Rev. **110**, 927 (1958).

[2] There are many versions of the optical model, which differ essentially only in degree of elaboration and in choice of parameters. See, e.g., H. A. Bethe, Phys. Rev. **47**, 747 (1935); S. Fernbach, R. Serber, and T. B. Taylor, Phys. Rev. **75**, 1352 (1949); H. Feshbach, C. E. Porter, and V. F. Weisskopf, Phys. Rev. **90**, 166 (1953), and Phys. Rev. **96**, 448 (1954); and F. E. Bjorklund and S. Fernbach, Phys. Rev. **109**, 1295 (1958). We shall usually refer to that of Bjorklund and Fernbach, which we regard to be the most complete and most successful.

[3] R. K. Smith, L. Cranberg, and J. S. Levin, Bull. Am. Phys. Soc. 4, 218 (1959).

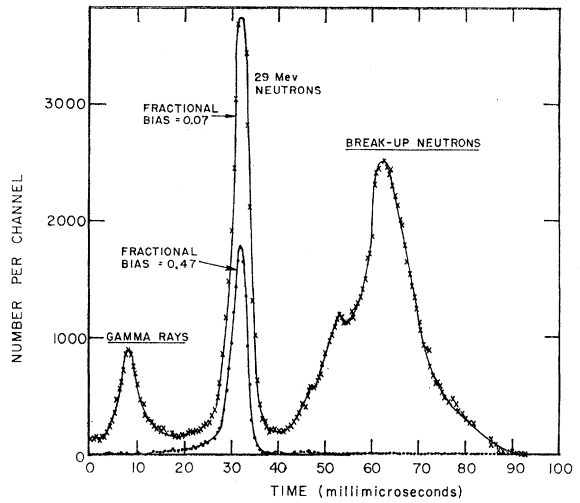

FIG. 1. Time-of-flight spectrum of the nominal 29-Mev neutron beam produced by 11-Mev deuterons striking a thin tritium gas target and detected by a biased plastic scintillator. Zero on the time scale corresponds to the time of the cyclotron beam pulse striking the tritium target.

detected "good" neutrons as a function of fractional bias (Figs. 2 and 3). When the bias is set near 60% of the neutron maximum pulse height, the ratio of the detected gamma rays to the detected good neutrons is less than 0.3% at every energy. Also, at this bias setting the ratio of the detected breakup neutrons to detected good neutrons is about 0.7% at 29 Mev and completely negligible at the two lower energies. This consideration is not applicable at 17 Mev since the incident deuteron energy is below the threshold energy for breakup. The error in total cross section corresponding to a 1% breakup neutron contribution amounts to about 0.3% in the worst case at 29 Mev. From these considerations a low fractional bias point of 60% was chosen for neutron energies of 17, 20, and 29 Mev. At 25 Mev the bias level was set at 55%. A high fractional bias of 85% also was used to provide both a means of compensating for electronic gain changes via the "window" method (see Appendix I of P7-14) and a means of detecting changes in neutron energy and electronic gain. As a means of checking discriminator stability, three identical discriminator scalers were used at each low bias and two at each high bias. Under normal cyclotron beam current the typical open-beam detector counting rate is about 100 counts/sec at the low bias levels.

One sample run sandwiched between two open beam runs furnishes the data for one determination of cross section. Each sample is run several times at each energy. The background is similarly determined using a copper sample 18 in. in length, whose transmission is less than 10^{-4} at each energy.

The mean deuteron energy is determined by making a differential range measurement, as described in

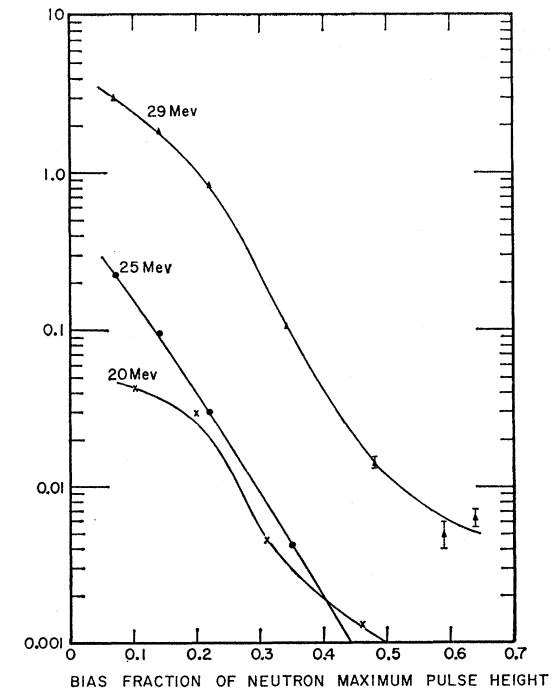

FIG. 2. Ratios of the number of detected breakup neutrons to the number of detected "good" neutrons from the *d*-T reaction as functions of the relative bias on the plastic scintillator for three nominal neutron energies.

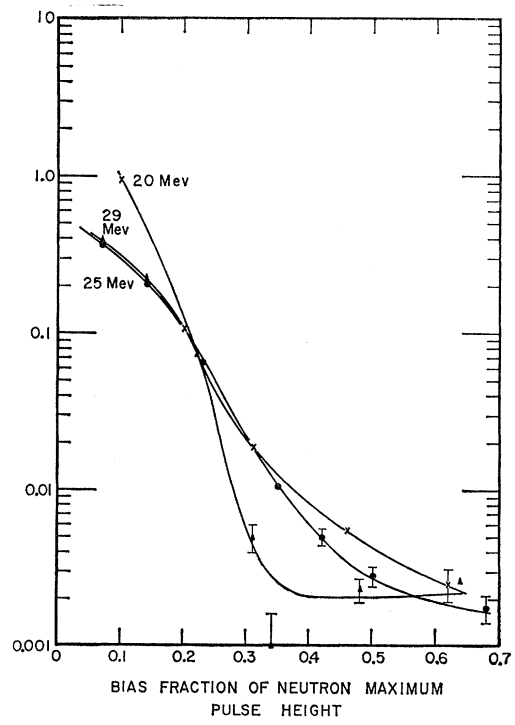

FIG. 3. Ratios of the number of detected gamma rays to the number of detected "good" neutrons as functions of the relative bias on the plastic scintillator for three nominal neutron energies.

TABLE I. Total cross sections in the 17- to 29-Mev range.

Element	E_n (Mev)	σ_t (barns)	E_n (Mev)	σ_t (barns)	E_n (Mev)	σ_t (barns)	E_n (Mev)	σ_t (barns)
H	17.8	0.560±0.009	20.6	0.47±0.01	25.3	0.388±0.009	28.3	0.34 ±0.01
							29.0	0.331±0.008
D	17.8	0.686±0.008	20.6	0.60±0.01	25.3	0.513±0.009	29.0	0.440±0.007
Li^6	18.1	1.24 ±0.02	20.4	1.15±0.01	25.3	1.01 ±0.01	27.7	0.94 ±0.01
Li^7	18.1	1.27 ±0.02	20.4	1.18±0.01	25.3	1.05 ±0.01	27.7	0.97 ±0.02
Be	17.5	1.39 ±0.01	20.5	1.31±0.01	25.3	1.19 ±0.01	27.9	1.15 ±0.01
C	17.8	1.42 ±0.01	20.6	1.46±0.01	25.3	1.38 ±0.01	28.3	1.32 ±0.02
							29.1	1.32 ±0.01
N	17.7	1.54 ±0.02	20.6	1.52±0.03	25.3	1.41 ±0.02	29.1	1.41 ±0.02
O	18.0	1.60 ±0.02	20.8	1.69±0.03	24.0	1.65 ±0.02	27.6	1.61 ±0.02
F	17.7	1.75 ±0.02	20.6	1.77±0.03	25.3	1.77 ±0.02	29.1	1.75 ±0.02
Mg	17.5	1.81 ±0.01	20.7	1.81±0.01	25.3	1.84 ±0.03	27.6	1.87 ±0.02
Al	18.0	1.78 ±0.02	20.7	1.81±0.02	24.2	1.85 ±0.02	27.7	1.91 ±0.02
					25.3	1.88 ±0.02		
Si	18.0	1.84 ±0.02	20.8	1.94±0.03	24.0	1.89 ±0.02	27.6	2.00 ±0.03
Ca	18.1	2.09 ±0.02	20.4	2.11±0.03	25.3	2.15 ±0.02	27.7	2.20 ±0.03
Ti	17.5	2.19 ±0.02	21.4	2.17±0.02	25.1	2.24 ±0.03	28.6	2.31 ±0.03
V	17.5	2.16 ±0.02	20.4	2.10±0.03	24.1	2.18 ±0.02	27.7	2.27 ±0.03
Cr	17.5	2.23 ±0.02	21.4	2.17±0.02	25.1	2.18 ±0.02	28.6	2.27 ±0.03
Fe	17.3	2.35 ±0.03	21.4	2.23±0.02	25.1	2.26 ±0.03	27.8	2.30 ±0.02
Co	17.4	2.45 ±0.03	21.4	2.34±0.03	25.3	2.32 ±0.03	29.0	2.41 ±0.03
Ni	17.5	2.44 ±0.02	21.4	2.31±0.03	25.1	2.31 ±0.02	28.6	2.37 ±0.03
	18.4	2.40 ±0.03						
Cu	17.4	2.62 ±0.02	20.5	2.48±0.03	24.1	2.41 ±0.02	27.6	2.46 ±0.03
	18.1	2.58 ±0.03	21.4	2.46±0.03	25.2	2.41 ±0.02	28.3	2.46 ±0.03
							29.0	2.45 ±0.02
Zn	17.5	2.75 ±0.03	21.4	2.58±0.03	25.1	2.49 ±0.03	28.6	2.52 ±0.03
Ga	17.6	2.87 ±0.05	21.4	2.65±0.03	25.3	2.56 ±0.04	28.6	2.56 ±0.04
Ge	17.5	2.94 ±0.03	21.4	2.69±0.03	25.1	2.61 ±0.02	28.9	2.61 ±0.03
Zr	17.4	3.55 ±0.04	20.5	3.31±0.04	25.2	2.92 ±0.03	28.9	2.87 ±0.03
Mo	17.3	3.66 ±0.04	21.4	3.27±0.03	24.1	3.14 ±0.04	27.7	2.98 ±0.04
					25.2	3.03 ±0.04	28.8	2.90 ±0.03
Pd	17.5	3.96 ±0.04	21.4	3.57±0.04	25.2	3.34 ±0.04	28.9	3.16 ±0.04
Ag	17.4	3.98 ±0.05	21.4	3.59±0.04	25.2	3.34 ±0.04	28.8	3.17 ±0.03
Cd	17.3	4.13 ±0.05	21.4	3.72±0.04	25.2	3.46 ±0.04	28.8	3.26 ±0.03
In	17.5	4.26 ±0.05	21.4	3.82±0.04	25.3	3.48 ±0.04	28.9	3.31 ±0.04
	18.4	4.12 ±0.05						
Sn	17.3	4.32 ±0.05	21.4	3.85±0.04	25.2	3.53 ±0.03	28.8	3.38 ±0.04
Sb	17.5	4.38 ±0.05	21.4	3.96±0.05	25.2	3.63 ±0.04	28.8	3.41 ±0.04
Ce	17.5	4.88 ±0.05	20.5	4.53±0.06	24.1	4.27 ±0.05	27.8	3.89 ±0.05
Ta	17.3	5.41 ±0.06	21.3	5.28±0.05	24.1	5.04 ±0.05	27.8	4.72 ±0.05
W	17.3	5.42 ±0.07	21.3	5.24±0.06	25.2	4.96 ±0.06	28.8	4.61 ±0.05
Pt	17.3	5.54 ±0.06	21.3	5.56±0.06	25.2	5.27 ±0.06	28.9	4.92 ±0.05
Au	17.3	5.63 ±0.06	20.3	5.70±0.07	25.2	5.31 ±0.05	27.7	5.10 ±0.05
							28.8	4.99 ±0.05
Tl	17.5	5.78 ±0.06	21.3	5.70±0.06	25.2	5.54 ±0.05	28.9	5.22 ±0.06
Pb	17.3	5.77 ±0.07	20.3	5.91±0.06	25.1	5.56 ±0.07	28.8	5.37 ±0.05
Bi	17.3	5.82 ±0.06	21.3	5.85±0.06	25.1	5.64 ±0.07	28.9	5.39 ±0.06
U^{235}	17.3	6.06 ±0.07	21.3	6.17±0.09	25.1	6.08 ±0.07	28.9	5.79 ±0.05
U^{238}	17.3	6.04 ±0.07	21.3	6.18±0.06	25.1	6.05 ±0.07	28.9	5.81 ±0.06
Pu	17.3	6.08 ±0.07	21.3	6.19±0.08	25.1	6.10 ±0.07	28.9	5.87 ±0.06

P7-14, and the corresponding neutron energies are found from the tables of Fowler and Brolley.[4] The uncertainty in the mean neutron energy due to uncertainties in range measurements varies from ±1.5% at 17 Mev to about ±0.7% at the higher energies. In the vicinity of 17 Mev, where the 4-in. gas target is filled to one-half atmosphere of tritium, the neutron energy spread due to gas target thickness is ±1.5%, and at the higher energies, where one atmosphere of tritium is used, it varies from ±0.7% to ±0.3%. In addition, there is an inherent energy spread in the deuteron beam from the cyclotron which contributes at most ±0.3% spread in the neutron energy.

[4] F. L. Fowler and J. E. Brolley, Revs. Modern Phys. 28, 103 (1956).

RESULTS AND DISCUSSION

A. Results

The measured neutron total cross sections of 42 elements and isotopes between 17 and 29 Mev are tabulated in Table I. Corrections for background, in-scattering, and chemical and isotopic composition have been applied. These data are plotted in Fig. 4 along with other data[5] going down to 1 Mev. This plot shows that the new data represent a smooth extension

[5] Our older data[1] are used between 7 and 14 Mev. Below 7 Mev various sources were used as referenced in *Neutron Cross Sections*, compiled by D. J. Hughes and R. Schwartz, Brookhaven National Laboratory Report BNL-325 (Superintendent of Documents, U. S. Government Printing Office, Washington, D. C., 1958), 2nd ed.

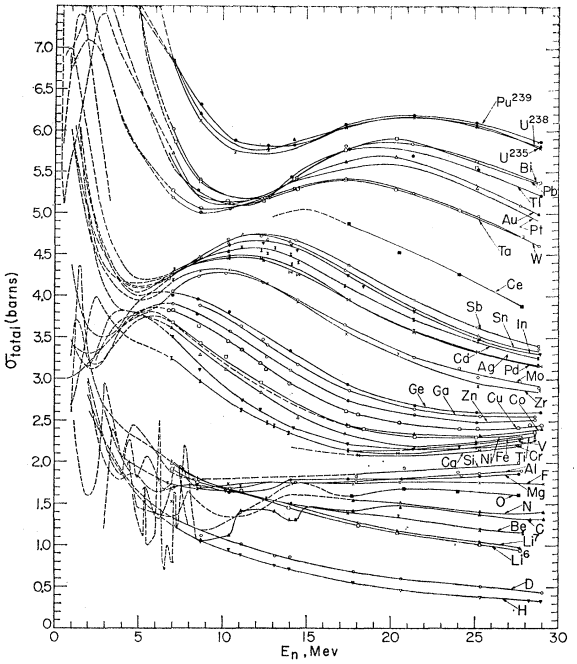

FIG. 4. Plots of measured total cross sections for many elements from 1 to 29 Mev. The solid curves represent Livermore data; the dashed curves were obtained from the neutron compilation (see reference 5).

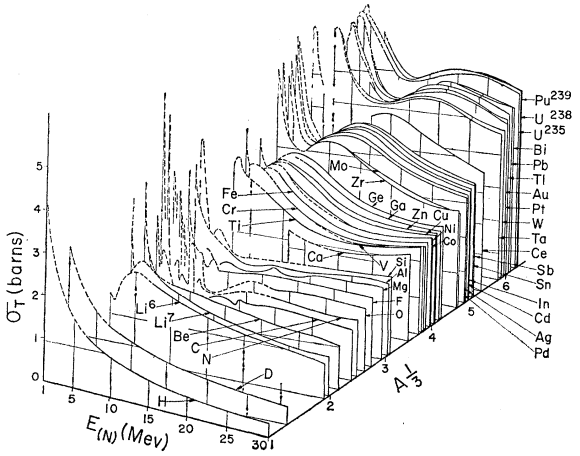

FIG. 5. Three-dimensional model of the 1- to 29-Mev total cross-section data shown in Fig. 4. Cross section is plotted versus neutron energy and $A^{\frac{1}{3}}$.

of the older data and that altogether they form a smooth cross section surface, as would be expected on the basis of the optical model, except in the region of low mass number at low neutron energies, where resonant structure is evident. These same data are shown in Fig. 5 which is a three-dimensional, Barschall-type[6] plot of total cross section versus neutron energy versus $A^{\frac{1}{3}}$, A being the mass number.

B. Comparison with Existing Data

The agreement of these data with older data is generally good. At 29 Mev there are three measurements of Taylor and Wood[7] which can be compared with ours. All three are in agreement with our data. At 25 Mev there are 6 measurements of Sherr[8] in agreement with our data, and none in disagreement. In the 19- to 20-Mev region there are 11 measurements of Day and Henkel[9] which are in agreement, and none in disagreement, although in one case (zirconium) the errors barely overlap.

The comparison with existing data in the energy region 15 to 18 Mev is more complicated because several independent sets of data exist, among which there are often disagreements. With the Conner[10] data we have 6 cases of agreement and no disagreements. With the Vervier[11] data we have 7 agreements and 2 disagreements. With the Mazari[12] data there are 6 agreements and 3 disagreements. With the Cook and Bonner[13] data, 4 agreements and 3 disagreements. With the Khaletskii[14] data, 3 agreements and 9 disagreements. In no case do we disagree with a previous worker without simultaneously agreeing with someone else. In addition, our data join on smoothly in every case with our older data in the 7- to 14-Mev region. For 13 elements no data existed with which to compare our results at any point in the 15- to 30-Mev interval. After examining these comparisons in detail we conclude that there is generally agreement with the older data, which is relatively sparse, and no serious disagreement.

In addition, we find good agreement where we overlap with the recent data of Dr. J. J. Thresher, who very kindly showed us his results before publication. Using the Harwell cyclotron, Thresher has measured the total cross sections of C, Al, Cu, Cd, and Pb between 16.5 and 117.5 Mev.

C. Errors and Uncertainties

The over-all errors assigned to each cross section are given in Table I. The statistical error is typically about 0.5% and is usually the dominant term in the over-all error. The background varied from about 2.5% at 17 Mev to 2.7% at 29 Mev and was known to within about one part in 50. The in-scattering correction was made according to the formula developed in Appendix II of P7-14, in which the ratio of the elastic scattering cross section at zero degrees to the total cross section

[6] H. H. Barschall, Phys. Rev. **86**, 431 (1952).
[7] A. E. Taylor and E. Wood, Phil. Mag. **44**, 95 (1953).
[8] R. Sherr, Phys. Rev. **68**, 240 (1945).
[9] R. B. Day and R. Henkel, Phys. Rev. **92**, 358 (1953).
[10] J. P. Conner, Phys. Rev. **109**, 1268 (1958).
[11] J. F. Vervier and A. Martegani, Phys. Rev. **109**, 947 (1958).
[12] M. Mazari, F. Alba, and V. Serment, Phys. Rev. **100**, 972(A) (1955).
[13] C. F. Cook and T. W. Bonner, Phys. Rev. **94**, 651 (1954).
[14] M. M. Khaletskii, Doklady Akad. Nauk S.S.S.R. **113**, 305 (1957) [translation: Soviet Phys.-Doklady **2**, 129 (1957)].

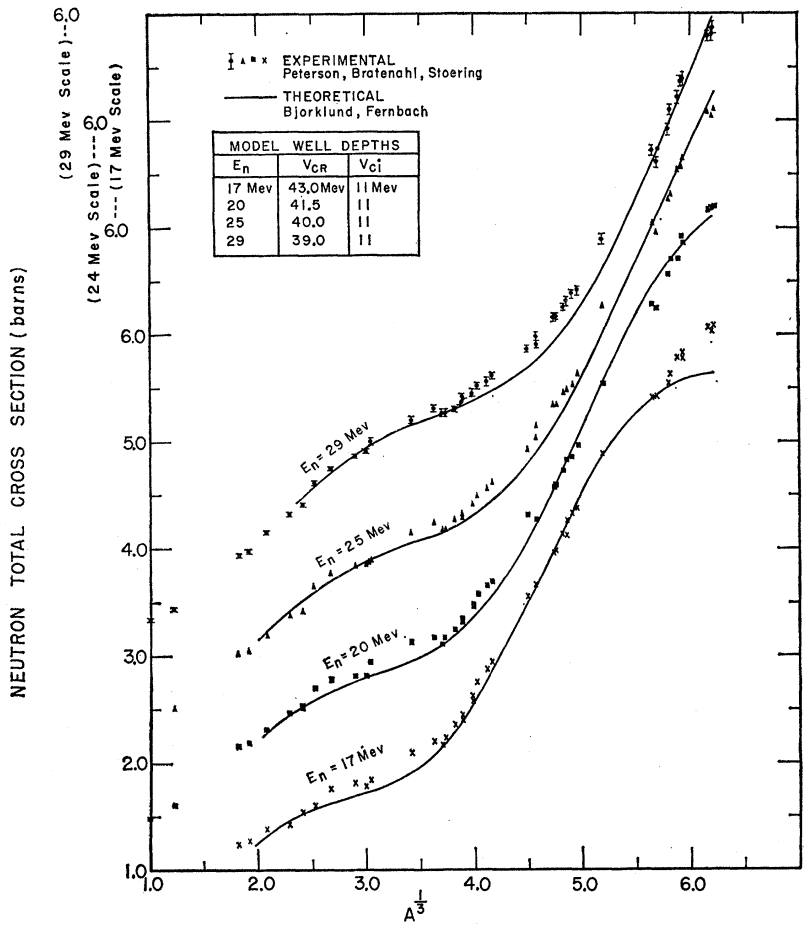

FIG. 6. Comparison of experimental and theoretical total cross sections at four energies. The experimental values are shown as points; the optical-model calculations of Bjorklund and Fernbach are shown as solid curves.

was approximated as $(kR+1)^2/8\pi$, where k is the neutron wave number and R is the nuclear radius, taken as $1.4A^{\frac{1}{3}}$ fermis. This recipe was verified to hold in the 17- to 29-Mev energy region, as well as the 7- to 14-Mev region, by comparing it with the ratio computed using the measured angular distribution at 24 Mev of Stuart and co-workers[15] for iron and bismuth. Here the recipe held to within 20% of the measured ratio and so it was applied throughout with confidence. Because of the rather good geometry employed, the in-scattering correction was always quite modest. In the worst case (plutonium at 29 Mev) it amounted to only 1.3% in the final cross section, and in most cases it was 0.5% or less.

Random errors from sources other than counting statistics are most likely to arise from short-time changes in the gain of the electronic system and/or the energy of the deuteron beam. These effects were watched for by monitoring the reproducibility of the ratio of the high to the low bias counts of each detector, which is sensitive to both of these effects; no serious drifts were found.

[15] T. P. Stuart, J. D. Anderson, and C. Wong, Bull. Am. Phys. Soc. 4, 257 (1959).

Systematic errors from sources not already considered are difficult to assess. One source is the presence of contaminants and voids in the transmission samples. These were guarded against by extensive chemical analyses and x-ray and ultrasonic examination. Mass spectroscopy also was employed for analysis of our deuterium sample. Systematic errors can also be detected through internal comparisons of the data. Our 7- to 14-Mev data (in P7-14) were consistent with the assumption that the cross sections of the medium and heavy nuclei vary smoothly, both as functions of energy and as functions of mass number, even in the neighborhood of magic-number nuclei; this statement is true also with the 17- to 29-Mev data with one exception, that exception being on the plots of cross section versus $A^{\frac{1}{3}}$ where the cross sections of vanadium and chromium (especially vanadium) consistently dip away by about 5% from smooth curves through the rest of the data (Fig. 6). Since the principal isotopes of vanadium and chromium are both magic in having closed shells of 28 neutrons, it is tempting to attribute this effect to the closed shells. However, all of the other magic nuclei measured (Ca, Ni, Sn, Ce, Pb, and Bi) fit nicely onto a smooth curve through the data at

TABLE II. Optical-model well depths used.

E_n (Mev)	V_{CR} (Mev)	V_{CI} (Mev)
17	43	11
20	41.5	11
25	40	11
29	39	11

each energy, which leaves us without any obvious conclusion to draw regarding vanadium and chromium. Incidentally, vanadium was not included in the 7- to 14-Mev work, although chromium was included and did not deviate from the smooth curves at those energies. For the elements magnesium and heavier, 90% of the points in the present work lie within 2% of the smooth curves.

The errors assigned in Table I are compounded from reproducibility or statistics (whichever was the larger) plus an arbitrary 0.5%.

D. Comparison with Optical-Model Predictions

The experimental data are compared with the theoretical predictions of the optical model of Bjorklund and Fernbach[2] in Fig. 6, the experimental data being shown as points and the theory as a solid curve at each energy. The optical model represents the interaction $V(r)$ between the neutron and the nucleus of mass A as a rounded, attractive, real potential well of depth V_{CR} and radius R plus an imaginary (absorptive) well of Gaussian shape with depth V_{CI} centered at R plus a real spin-orbit potential, as follows:

$$V(r)=V_{CR}\rho(r)+iV_{CI}g(r)+V_{SR}\left(\frac{\hbar}{\mu c}\right)^2\frac{1}{r}\frac{d\rho(r)}{dr}\boldsymbol{\sigma}\cdot\mathbf{l},$$

where $\rho(r)=[1+e^{(r-R)/a}]^{-1}$, $g(r)=\exp\{-[(r-R)/b]^2\}$, $R=r_0a^{\frac{1}{3}}=1.25\,A^{\frac{1}{3}}$ fermi, $a=0.7$ fermi, $b=1.0$ fermi, $\hbar/\mu c$=pion Computon wavelength, $\boldsymbol{\sigma}$=neutron spin vector, and $\mathbf{l}$=angular momentum vector of the lth partial wave. The spin-orbit potential used is based on that necessary to predict the correct angular distributions at 14 and 24 Mev and is included here although the total cross-section predictions are not sensitive to it. The depths of the real and imaginary wells used for the curves in Fig. 6 are given in Table II. Figure 6 shows that the Bjorklund-Fernbach optical model fits the experimental total cross-section data fairly well, even for elements as light as beryllium at these energies, despite the fact that the curves do not have simple mass and energy dependence. In most cases the predicted cross sections are within a few percent of the measured values, but in some regions the discrepancy is as high as 10%. The well depth parameters can be determined in this way to within about ±1 Mev for a given nuclear radius constant r_0, which Bjorklund and Fernbach gives as 1.25±0.05 fermi. The total cross-section curves are not as sensitive to the depth of the imaginary well as to the depth of the real well, and the imaginary depth cannot be determined in this way to better than ±3 Mev. The well depths in Table II are consistent with the energy dependence given by Bjorklund and Fernbach.[16]

TABLE III. Corrected total cross sections for tungsten in the 7- to 14-Mev range.

E_n (Mev)	7.05	8.67	10.3	12.3	14.3
σ_t (barns)	5.19±0.05	5.00±0.04	5.06±0.05	5.18±0.05	5.30±0.06

E. Conclusions and Interpretations

We have seen that the experimental total cross-section data in the 7- to 29-Mev region are fitted quite well by optical model analysis and help to determine the energy dependence of the model's parameters. In addition, they map out a smooth ridge of maxima in the total cross-section surface (Figs. 4 and 5) which extends from, say, chromium at 4 Mev up to plutonium at about 20 Mev; furthermore, they even hint at another ridge at higher energies. Such "neutron giant resonances" are well known[17] and have been interpreted[2,18] usually in terms of single-particle resonances. We find, however, that the single-particle resonance interpretation cannot explain these neutron giant resonances. Yet, they can be successfully interpreted in terms of a nuclear Ramsauer effect, in which a maximum in cross section occurs when the neutron is at such an energy that the wave which traverses the nucleus emerges exactly out of phase with the wave which goes around the nucleus. Other ridges of neutron giant resonances at higher and lower energies can be similarly interpreted. This nuclear Ramsauer effect is discussed in a paper now being prepared.

CORRECTION TO PREVIOUS DATA

While carrying out the present work it was found that the composition of our tungsten sample was somewhat different from that used to reduce our data in the 7- to 14-Mev region. As a result the total cross sections for tungsten reported in P7-14 are in error and should be corrected to the values shown in Table III.

ACKNOWLEDGMENTS

We wish to thank the many people who have helped with this work. They include H. Catron, Barbara Hurlbut, Marinda Kelley, R. Lingenfelter, who helped in running the experiment and data analysis, F. E. Bjorklund and S. Fernbach, who did the optical model work, and D. Rawles, A. Horn, D. Malone, and H. Fong of the cyclotron crew.

[16] F. E. Bjorklund and S. Fernbach, University of California Radiation Laboratory Report UCRL-5028, 1958 (unpublished).

[17] N. Nereson and S. Darden, Phys. Rev. **89**, 775 (1953), and Phys. Rev. **94**, 1678 (1954).

[18] A. M. Lane, R. G. Thomas and E. P. Wigner, Phys. Rev. **98**, 693 (1955); S. G. Carpenter and R. Wilson, Phys. Rev. **114**, 510 (1959).